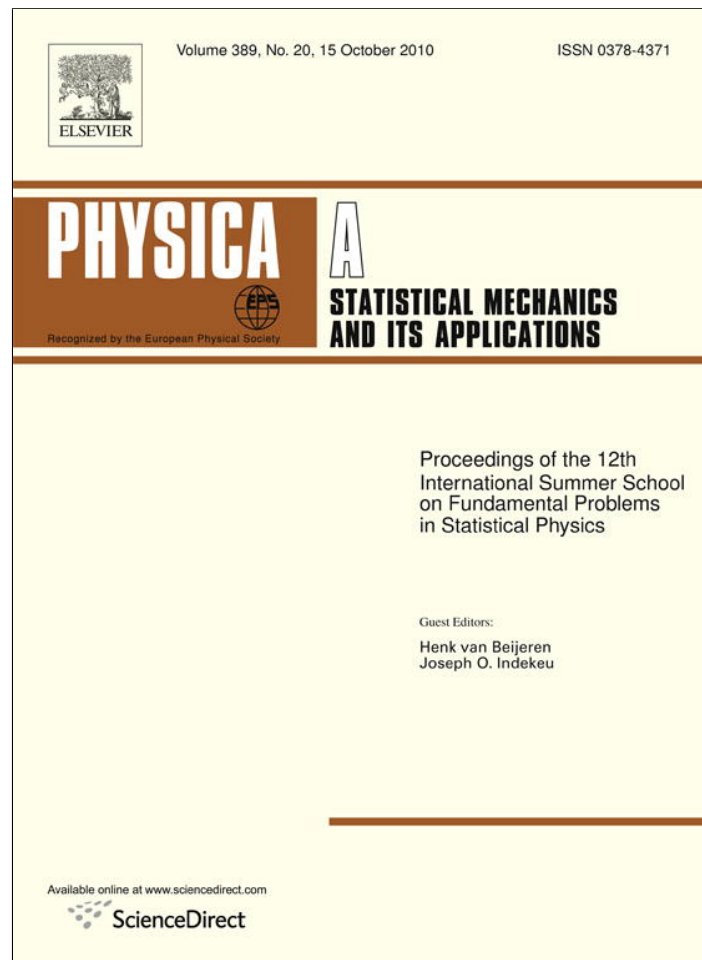


Provided for non-commercial research and education use.
Not for reproduction, distribution or commercial use.



This article appeared in a journal published by Elsevier. The attached copy is furnished to the author for internal non-commercial research and education use, including for instruction at the authors institution and sharing with colleagues.

Other uses, including reproduction and distribution, or selling or licensing copies, or posting to personal, institutional or third party websites are prohibited.

In most cases authors are permitted to post their version of the article (e.g. in Word or Tex form) to their personal website or institutional repository. Authors requiring further information regarding Elsevier's archiving and manuscript policies are encouraged to visit:

<http://www.elsevier.com/copyright>



Contents lists available at ScienceDirect

Physica A

journal homepage: www.elsevier.com/locate/physa

Jamming: A simple introduction

Alexander O.N. Siemens*, Martin van Hecke

Kamerlingh Onnes Laboratory, Leiden University, PO Box 9504, 2300 RA Leiden, The Netherlands

ARTICLE INFO

Article history:

Received 12 December 2009

Received in revised form 18 February 2010

Available online 26 February 2010

Keywords:

Jamming

Amorphous materials

Disordered materials

ABSTRACT

Amorphous materials as diverse as foams, emulsions, colloidal suspensions and granular media can *jam* into a rigid, disordered state where they withstand finite shear stresses before yielding. Here we give a simple introduction to the surprising physics displayed by a very simple model system for the jamming transition: frictionless, soft spheres at zero temperature and zero shear that act through purely repulsive contact forces. This system starts to become rigid, i.e. goes through the jamming transition, whenever the confining pressure becomes positive. We highlight some of the remarkable geometrical features of the zero pressure jamming point and discuss the peculiar mechanical properties of these systems for small pressures.

© 2010 Elsevier B.V. All rights reserved.

1. Overview

Many everyday materials, such as sand, toothpaste, mayonnaise, and shaving foam, exhibit an intriguing mix of liquid-like and solid-like behaviors, some familiar, some surprising, but often poorly understood. What all these materials have in common is that they consist of disordered collections of macroscopic constituent particles: sand is a dense packing of solid grains (Fig. 1(a)), toothpaste is a dense packing of (colloidal) particles in fluid (Fig. 1(b)), mayonnaise is an emulsion consisting of a dense packing of (oil) droplets in an immiscible fluid (Fig. 1(c)), and shaving foam is a dense packing of gas bubbles in fluid (Fig. 1(d)).

Dense is the keyword here—these materials obtain finite rigidity once their constituent particles are brought in contact. Nevertheless, all these materials can be made to flow by the application of relatively small stresses—in fact their utility often stems from precisely this combination of liquid-like and solid-like behavior. By varying thermodynamic (temperature or density) and mechanical (applied stress) variables, one can bring about a transition from a freely flowing to a *jammed* state in many other disordered media. An increase in the density causes colloidal suspensions to turn glassy. Similarly, flowing foams can be made static by decreasing the applied stress to below the yield stress. In 1998, Liu and Nagel presented a novel way of understanding jamming through a phase diagram (Fig. 1(e)) and proposed to probe various transitions to rigidity [1].

This review aims at giving a basic introduction to our current understanding to the following two questions: What is the nature of the jammed state? What is the nature of the jamming transition? We will illustrate the main features of these systems by idealized pictures demonstrating our current understanding rather than “real” experimental and numerical data. For a more elaborate introduction, the reader is referred to two more detailed reviews paper and references therein [2,3].

We will deal only with zero temperature packings of frictionless soft spheres that interact through purely repulsive contact forces. “Soft” in this case means that the individual particles can be deformed under relevant loads—deformations are key. We review the geometrical and mechanical properties of these systems as a function of the distance to jamming.

2. Jamming in a simple model

Over the last decade, tremendous progress has been made in our understanding of what might be considered the “Ising model” for jamming: static packings of soft, frictionless spheres that act through purely repulsive contact forces. In this

* Corresponding author.

E-mail address: siemens@physics.leidenuniv.nl (A.O.N. Siemens).

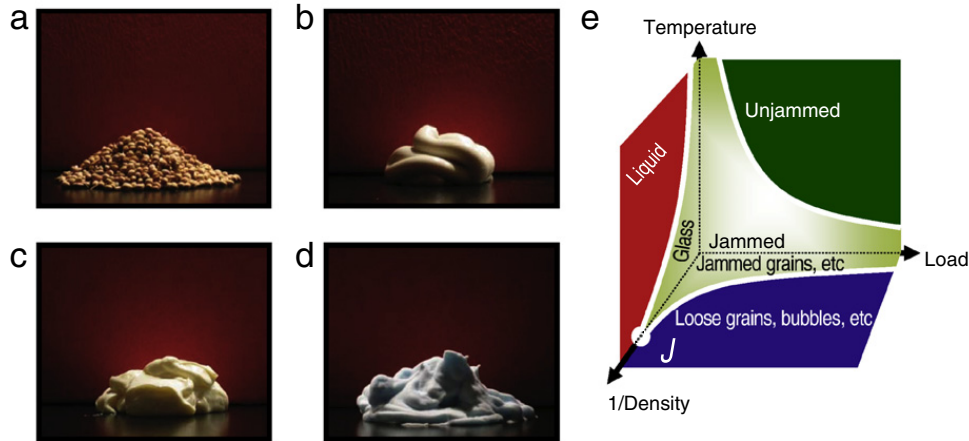


Fig. 1. (a–d) Examples of everyday disordered media in a jammed state. (a) Granular media. (b) Toothpaste. (c) Mayonnaise. (d) Shaving foam. (e) Jamming diagram as proposed by Liu, Nagel and co-workers [1,4]. The diagram illustrates that many disordered materials are in a jammed state for low temperature, low load and large density, but can yield and become unjammed when these parameters are varied. In this review we will focus on the zero temperature and zero load axis. For frictionless soft spheres, there is a well-defined jamming transition indicated by point “J” on the inverse density axis, which exhibits similarities to an (unusual) critical phase transition.

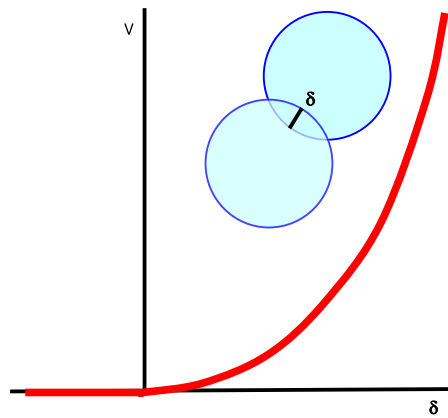


Fig. 2. The interaction potential V for pairs of interacting soft frictionless spheres is a simple function of the particles overlap, δ , only.

model, temperature, gravity and shear are set to zero. The beauty of such systems is that they allow for a precise study of a jamming transition. In this section we introduce this model and discuss some aspects of its jamming transition and its main parameters.

2.1. Model

The most studied and best understood model for jamming consists of soft spherical particles that only interact when in contact—with the interaction forces set by the amount of virtual overlap between two particles in contact. Moreover, the contact forces are purely repulsive—no frictional forces and no attraction are included.

Denoting the undeformed radii of particles in contact as R_i and R_j and the center-to-center distance as r_{ij} , it is convenient to define a dimensionless overlap parameter δ_{ij} as

$$\delta_{ij} := 1 - \frac{r_{ij}}{R_i + R_j}, \tag{1}$$

so that particles are in contact only if $\delta_{ij} \geq 0$. Since we only will study static properties here, there is no need for specifying a dissipative mechanism.

Power law interaction potentials take on the form (see Fig. 2):

$$\begin{aligned} V_{ij} &= \delta_{ij}^\alpha \quad \delta_{ij} \geq 0, \\ V_{ij} &= 0 \quad \delta_{ij} \leq 0. \end{aligned} \tag{2}$$

For harmonic interactions, $\alpha = 2$, while Hertzian interactions (the nonlinear contact laws for elastic spheres in 3D) correspond to $\alpha = 5/2$. O’Hern et al. have also studied the “Hernian” interaction ($\alpha = 3/2$), which corresponds to contacts that weaken progressively when compressed [4]. By varying the exponent α , the nature and robustness of various scaling laws can be probed, as we will see.

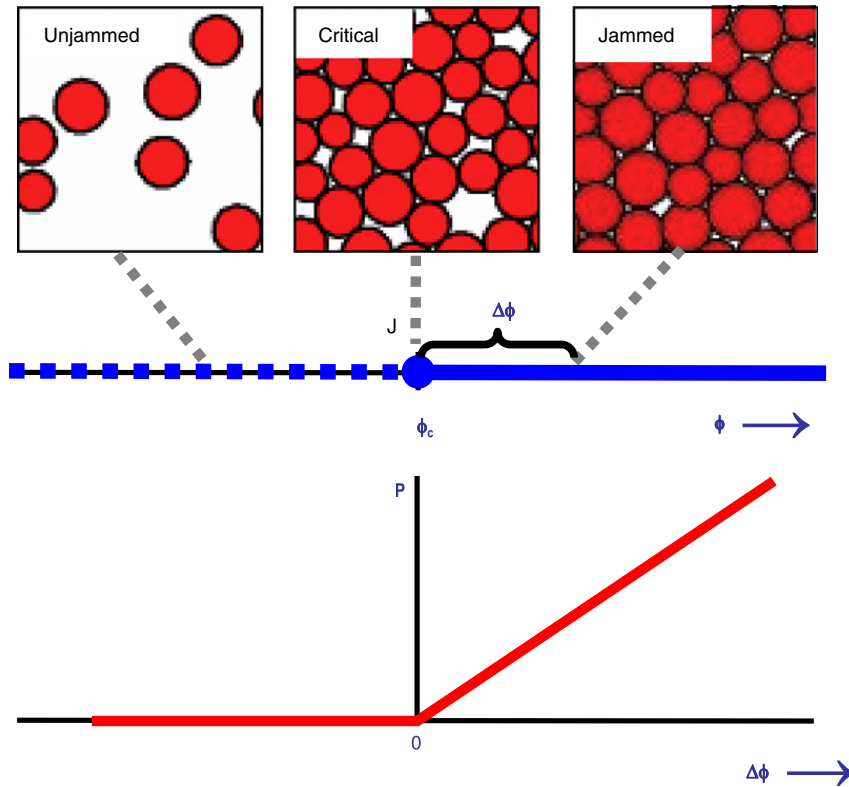


Fig. 3. Top: examples of repulsive soft particles below, at and above the jamming transition. The jamming point for frictionless soft spheres is referred to as point J . The packing density ϕ controls the transition here, and the jamming transition occurs at the critical value ϕ_c . The distance to jamming is given by the excess density $\Delta\phi$. Bottom: when the particles have simple harmonic interactions (when they overlap), the pressure grows linearly with excess density.

2.2. The jamming point

What is the jamming transition for this simple system? The main features are illustrated in Fig. 3. As the packing density of the particles, ϕ , is increased, the jamming transition occurs when essentially all particles start to touch but still are at zero pressure—this is called *point J*. Here ϕ_c , the critical packing fraction, is the point at which the particles start touching. The distance to the jamming point is often measured as $\Delta\phi = \phi - \phi_c$ —see Fig. 3 [4].

An alternative measure of the distance to jamming is the pressure in the system. If the particles are not in contact, the contact forces between the particles are zero, and so is the pressure. Once particles start to overlap, contact forces arise, and the pressure becomes non-zero (see Fig. 3). In fact, one can show that the pressure and the contact forces scale similarly— $P \sim \langle f \rangle$, where brackets denote the average over the system. For the simple interactions used here, there cannot be a finite force in part of the system, while other parts of the system are at zero pressure—hence, for finite pressure, the vast majority of particles experience finite contact forces (typically a few percent of the particles are *rattlers*, particles that have only zero contact forces).

Once the pressure is non-zero, the system is jammed. With this we mean that, first, the system has finite elastic moduli, so that applying infinitesimally small forces to the system leads to a proportional and reversible deformation. Second, the system has a finite yielding threshold: if we force the system so much that irreversible deformations arise, the amount of force is *finite* [4].

There are three important things to note: first, for finite systems, the jamming density ϕ_c varies between realizations—this is why one measures the distance to jamming with $\Delta\phi$ and not by ϕ . A disadvantage of using the excess density is that one must first obtain a value for ϕ_c . For simulations this can be done by starting with a jammed system and deflating the particle until the system is not rigid anymore [4]. This step is not necessary when the pressure is a control parameter, since at point J , $P = 0$.

To relate $\Delta\phi$ and P , we first note that the typical particle overlap δ scales as $\Delta\phi$. To relate the pressure and the typical particle overlap, we note that $P \sim f$, and that the force is just $f = -\nabla V_{ij}$. For power law interactions of the form Eq. (2), the potential is a function of the overlap, and hence we can relate $\Delta\phi$ and P as follows:

$$P \sim f = \frac{dV_{ij}}{d\delta} \sim \delta^{\alpha-1} \sim (\Delta\phi)^{\alpha-1}. \tag{3}$$

As is illustrated in Fig. 4, quantities measured as function of $\Delta\phi$ and as function of P can be directly translated.

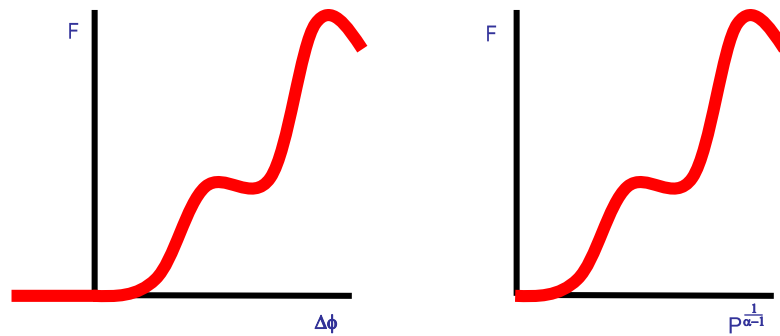


Fig. 4. Any function F of the excess packing density $\Delta\phi$ can be translated to a function of the pressure P —for power law interactions of the form Eq. (2), $P \sim (\Delta\phi)^{\alpha-1}$.

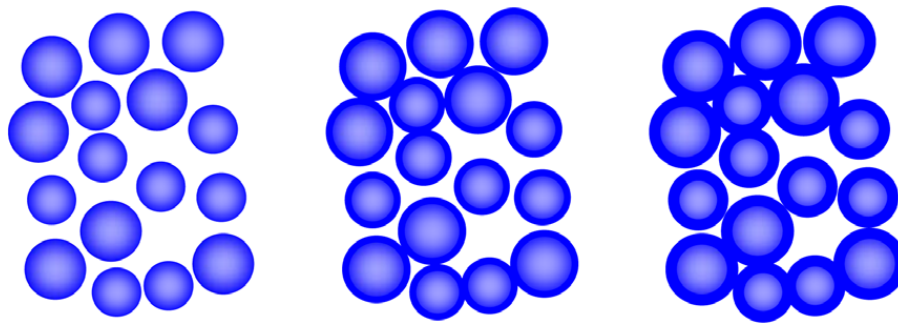


Fig. 5. An affine compression of a packing is equivalent to fixing the particles positions and then inflating their radii.

Second, infinitely hard, frictionless spheres will always remain at the jamming point for positive pressures, since their deformations are always zero. Many people are used to hard particles at *finite* temperature. To bring such particles in contact, one needs infinite pressure. It is useful to realize that hard particles at infinite pressure and finite temperature are equivalent to the zero pressure limit of soft, athermal particles.

Third, for infinite systems, ϕ_c tends to a well-defined value, directly related to *random close packing* of hard (undeformed) spheres. Random close packing is a notoriously tricky concept, since it is not always clear what random means. An attempt to model RCP based on experimental systems has only recently found some success [5]. In three dimensions, the densest possible packing is the regular FCC packing (similar to how oranges are packed in your grocery store), which reaches a packing density of 74%. What is now the densest random packing? This simple question defies a simple answer, since it is not immediately obvious what “random” means—for example, packings consisting of large FCC clusters that are irregularly stacked can attain densities arbitrarily close to the FCC density but still be called random. However, in the absence of any appreciable order, the densest random packings have $\phi_{RCP} \approx 0.64$ (in three dimensions—in two dimensions $\phi_{RCP} \approx 0.84$). Probing the jamming transition with a specific protocol may be seen as defining the RCP density [4].

3. Jammed materials are not ordinary solids

Superficially, the jamming transition appears similar to a liquid–solid-like transition such as freezing. Is the jammed phase simply a solid? In this section we will show that packings at or near jamming are very different from ordinary, *crystalline* solids. We will focus on the elastic and geometric properties of soft spheres near jamming. To highlight the anomalous behavior of jammed solids, we will first explicitly state what we think the simplest prediction for these properties would be. The simple predictions are essentially based on a picture where one ignores the disorder, so-called effective medium pictures, which would work well for ordered materials. As we will see, the essence of such pictures often is that one assumes deformations of the material to be affine, i.e., the local deformations follow trivially from the global.

The point is that such affine/effective medium predictions fail to describe disordered media and that the failure becomes increasingly pronounced when one approaches the jamming transition. Of course, this approach may appear like setting up a strawman argument, yet we feel it is a useful strategy to stress what is surprising about the jamming transition.

3.1. Contact number

A key parameter of a packing is its contact number, z , defined as the average number of contacts a particle has. How can we estimate z as function of packing fraction? Suppose we start with a low density situation where no particles touch. The simplest estimate of what happens when we compress such a packing is to assume that the local motion of the particles

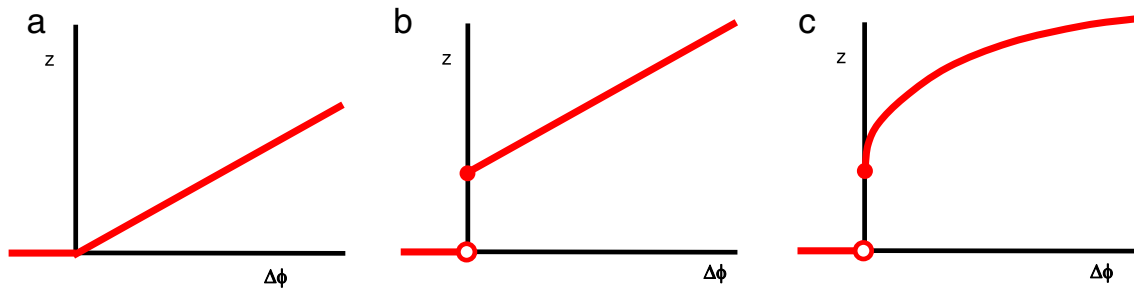


Fig. 6. The contact number as a function of the excess packing fraction. (a) In the most naive model, the contact number grows linearly with the packing fraction. (b) A more realistic model takes into account that there is a minimal contact number (the so-called isostatic value) and that the contact number at jamming jumps from 0 to $2d$. (c) In numerical simulations one finds that the contact number grows as the square root of the excess packing fraction above point J.

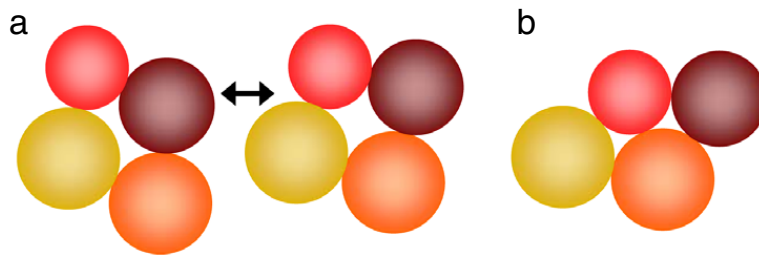


Fig. 7. (a) For low contact numbers, these packing can be deformed without deforming the particles—this is a (trivial) example of a floppy mode. (b) For sufficiently large contact numbers, there are no zero energy deformations of this packing possible—apart from trivial translations and rotations. Note that, of course, we could move particles away from another without energy cost. To make the counting more rigorous, one should consider packings with well-defined boundary conditions, which then prevents such problems.

simply follows the globally applied deformation—for compression this is equivalent to inflating all particle radii while keeping their position fixed (Fig. 5). More precisely, this uniform compression is an example of an *affine* deformation. A strict definition of affine transformations states that three collinear particles remain collinear and that the ratio of their distances is preserved, and affine transformations are, apart from rotations and translations, composed of uniform shear and compression or dilatation.

If the distribution of separations between the initial particles is regular, i.e. all separations occur with similar probability, the contact number grows smoothly from zero under affine compression (Fig. 6(a)). This simple model does not balance forces in the packing to make it stable, and as a consequence, the prediction for the growth of the contact number with packing density is far from the numerically observed growth (Fig. 6(c)).

The next step to take is to realize that stable packings can only exist once the contact number is above a minimum value, the so-called isostatic value, z_{iso} [6,7].

Suppose we have N soft frictionless spheres in d dimensions. The contact number equals z . The total amount of contacts in the packing is then $Nz/2$, since each contact is shared by two particles. For a packing to be stable, we require that it should not include floppy modes (which cost zero energy in the lowest order—see Fig. 7(a)). It can be shown that this is equivalent to demanding that the $Nz/2$ contact forces balance on all particles. For every particle we have d force constraints (force balance in the x -direction, y -direction and so forth), so force balance yields Nd constraints on $Nz/2$ force degrees of freedom. One generically expects solutions to such equations only when $z \geq 2d$. The isostatic contact number equals $z_{iso} = 2d$.

But wait, we are not done yet! At point J, the pressure is zero, so the particles are undeformed. The distance between two particles is therefore exactly the sum of their radii, giving $Nz/2$ constraints for the Nd positional degrees of freedom. The only trivial solutions are when $z \leq 2d$. Combining these two inequalities yields that at jamming, the contact number for frictionless spheres precisely equals $2d$.

We are now able to make another guess at how z should scale with $\Delta\phi$. If we were to now incorporate the balance of forces in our model, we would imagine that at point J, z would jump from 0 to 4 and then grow linearly for $\Delta\phi \geq 0$, as in Fig. 6(b). So what happens in simulations?

In 1997, Durian found that the contact number for a 2D system approaches $z = 4$ near jamming and that $z - 4$ scales non-trivially as the square root of the excess packing fraction above point J [8,4], $\Delta z \sim \sqrt{\Delta\phi}$. See Fig. 6(c). Most surprisingly, subsequent studies found that this relation is independent of the interaction potential and dimension.

Hence, the contact number already shows highly non-trivial behavior: first, it reaches a well-defined value at the jamming point, and second, it grows as a non-trivial power law above jamming. Most mechanical properties depend sensitively on z , and so we can already anticipate that the scaling of these will be surprising too.

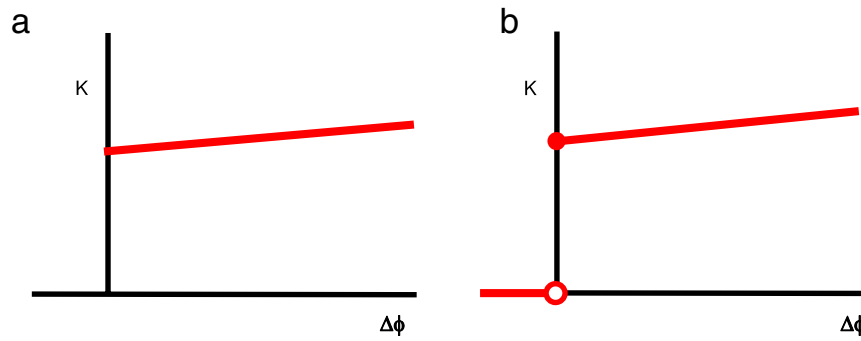


Fig. 8. The bulk modulus for packings with harmonic interactions, as a function of the excess packing fraction $\Delta\phi$ in the effective medium theory picture (a) and for simulations (b). In both cases, slight variations in the modulus with $\Delta\phi$ are expected due to an increase of the density of contacts with compression, but this does not influence the scaling behavior near $\Delta\phi = 0$.

3.2. Elastic moduli

The elastic moduli of disordered packings also show peculiar scaling with distance to the jamming point. When dealing with disordered media, the problem of how to take the disorder into account always arises. Ignoring disorder is an option, but then one can only describe ordered packings. A slightly more subtle approach is effective medium theory (EMT). EMT assumes that (i) macroscopic, averaged quantities can be obtained by a simple coarse graining procedure over the individual contacts and (ii) applying a global deformation trivially translates to changes in the local deformation. For example, a 1% strain on the entire sample will deform all the contacts between particles by 1%. This second assumption is the “affine assumption” [9].

Before confronting the predictions from EMT with direct numerical simulations, we have to briefly discuss the elasticity of individual contacts in our disordered packings. Under small deformations, a packing of soft, frictionless spheres is equivalent to a spring network, where each contact represents a spring. For a harmonic interaction potential, the spring constant is independent of the force—the spring constant of all contacts has the same value. For anharmonic potentials, such as the Hertzian and Hernian interactions discussed above, this is not true. One should realize that we start from an already compressed packing, and thus compressed contacts, and want to quantify what the effect is of additional small perturbations. The spring constant, k , is then given by

$$k = \frac{d^2V}{d\delta^2}, \quad (4)$$

where V is the potential, which typically is a power law function of the compression of the springs. Indeed we find for harmonic interactions ($V \sim \delta^2$), the spring constant is independent of the particles deformation and that for general power law interactions ($V \sim \delta^\alpha$), the spring constant scales as $k \sim \delta^{\alpha-2} \sim (\Delta\phi)^{\alpha-2}$.

3.2.1. Compression modulus

The compression modulus (or bulk modulus), K , determines the resistance of a disordered packing against homogenous compression. Under the affine assumption, for a global strain ϵ_{global} applied, this directly translates to the local strain ϵ_{local} felt by all particles. The changes in contact force then scale as $k\epsilon_{\text{local}} \sim k\epsilon_{\text{global}}$, which tells us that the elastic modulus is of order k : the elastic moduli follow the typical stiffness of the contacts. Therefore, $K \sim (\Delta\phi)^{\alpha-2}$ [4,10,11].

Numerical simulations on disordered packings are consistent with this: the affine assumption works well for compression—although, as we will see later, this is a lucky coincidence. Of course, the elastic moduli are zero in unjammed packings, and there is, for $\alpha \leq 2$, a discontinuous jump of K in simulations—see Fig. 8.

3.2.2. Shear modulus

The shear modulus, G , determines the resistance of a disordered packing against pure shear. Following arguments similar as for the compression case, EMT predicts that the shear modulus scales as $G \sim (\Delta\phi)^{\alpha-2}$ [9,4,10,11].

Numerical simulations on disordered packings show a different scaling, however: the actual shear modulus scales as $G \sim (\Delta\phi)^{\alpha-3/2}$ [9,4,10,11]—see Fig. 9. Hence, close to jamming, the systems is much softer to shear deformations than to compressive deformations, and the ratio of G/K goes to zero, independent of interaction potential. In fact, making use of the scaling of $\Delta z \sim \sqrt{\Delta\phi}$, one can write this ratio as $G/K \sim \Delta z$.

3.3. Vibrations

The special nature of packings near the jamming point can also be probed by the vibrational modes and their associated density of states (DOS), $D(\omega)$, which gives the spectral density of modes as function of their frequency ω . For crystalline solids, the vibrational modes are plane waves, and the DOS can be obtained by counting the number of modes in shells

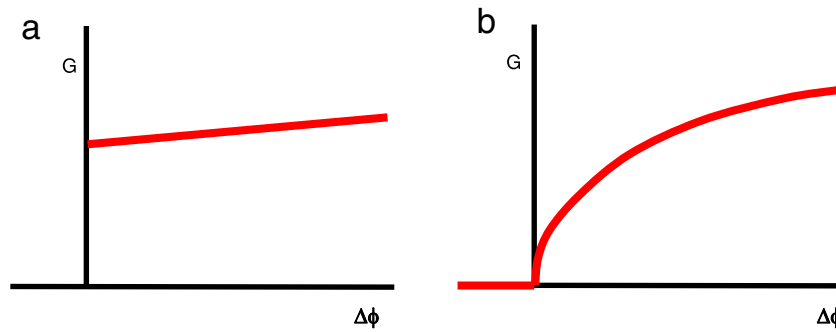


Fig. 9. The shear modulus for packings with harmonic interactions, as a function of the excess packing fraction $\Delta\phi$ in the effective medium theory picture (a) and for simulations (b). For shear, the affine assumption breaks down spectacularly.

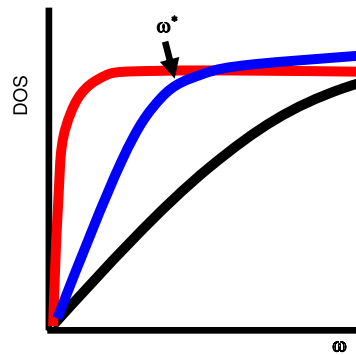


Fig. 10. The density of vibrational states as a function of the frequency of vibration in packings near jamming. For large distance to jamming (black curve), the low frequency behavior is consistent with the Debye behavior that $D(\omega) \sim \omega^{d-1}$. Closer to jamming (blue curve), there is an excess of low frequency modes, and the characteristic frequency ω^* shifts to lower frequencies. At jamming (red curve), ω^* reaches zero, and there is no trace left of ordinary Debye behavior. (For interpretation of the references to colour in this figure legend, the reader is referred to the web version of this article.)

of increasing frequency, as follows. Consider a square, periodic lattice in 2D. The wave vector κ takes on discrete values, $(\kappa_x, \kappa_y) = (nL/2\pi, ml/2\pi)$, where L is the size of the lattice and n and m are integers. Recall that the dispersion relation is written as $\omega = v\kappa$, where v is the velocity of sound. The total number of modes with frequency less than ω is then given by counting the “volume” in k -space of the sphere containing all wave numbers smaller than $\omega = v\kappa$:

$$N \sim (v\kappa)^2 \sim \omega^2. \tag{5}$$

The density of states is then $D(\omega) = dN/d\omega \sim \omega$. Similarly, one can find the DOS for arbitrary dimensions d : $D(\omega) \sim \omega^{d-1}$.

Frictionless packings show this Debye-like behavior at low ω and large P . When the pressure is lowered and one thus approaches the jamming transition, the DOS exhibit surprising features as illustrated in Fig. 10 [4,12,13]. The following picture emerges. First, far above jamming, the DOS for small frequencies is regular. Second, approaching point J, the DOS at low frequencies is strongly enhanced. More precisely, the DOS becomes essentially constant up to some low-frequency crossover scale at $\omega = \omega^*$, below which the continuum scaling $\sim \omega^{d-1}$ is recovered. Third, the characteristic frequency ω^* vanishes at point J as $\omega^* \sim \Delta z$. Hence, the closer one is to jamming, the less our jammed material appears to be similar to an ordinary crystalline solid. In addition, the vast majority of the eigenmodes do not appear as simple plane waves [14].

4. Beyond effective medium theory

In the previous section we have seen that the contact number, the elastic properties, and the vibrational spectra all signal the unique nature of materials near the jamming transition. In this section we briefly sketch *why* these materials behave so differently. We stress in particular the breakdown of the affine assumption in Section 4.1 below and return to the scaling of the contact number in Section 4.2.

4.1. Non-affine deformations

The anomalous scaling of the elastic moduli is related to the non-affine nature of the deformations of weakly jammed packings, although the precise connection is rather subtle. We will discuss our current understanding below.

An instructive way to illustrate the role of these non-affine deformations is to first force the particle displacements to be affine and then let them relax, while measuring the changes in the elastic energy (which are governed by the elastic moduli) in both cases.

O’Hern and co-workers found that the elastic moduli associated with the affine deformations scale precisely as predicted by effective medium theory. However, the forced system can lower its elastic energy by additional non-affine motion of

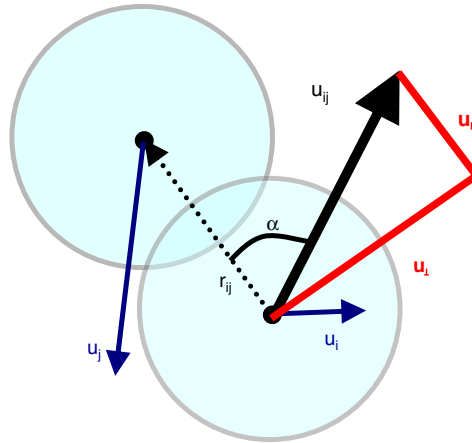


Fig. 11. Definition of the relative motion u_{ij} of two particles that each move by u_i and u_j respectively, and the corresponding $u_{||}$ and u_{\perp} .

the particles. These non-affine deformations are particularly strong for shear deformations, as they are found to change the scaling of the shear modulus [4].

It is tempting to conclude that the non-affinity then is stronger for shear deformations than for compressive deformations—however, subsequent studies found that both for shear and compression the non-affine deformations are large, and in fact diverge near jamming [10]. To characterize the local deformations, note that changes in elastic energy depend on the relative motion of pairs of contacting particles as

$$\Delta E = \frac{1}{2} \sum_{i,j} k_{ij} \left(u_{||,ij}^2 - \frac{\delta_{ij}}{\alpha - 1} u_{\perp,ij}^2 \right), \quad (6)$$

here $u_{||}$ and u_{\perp} are relative motions of particles parallel and perpendicular to each other, respectively (see Fig. 11). Note that u does not refer to flow, but to small, quasi-static displacements in response to external forcing. The u_{\perp} arises from applying Pythagoras theorem, and using Eq. (4) to related k and δ —see Ref. [2].

We now need a parameter to capture the degree of non-affinity, something that dictates how the system on a local scale responds to an imposed shear or compression as compared to an expected affine response. The probability distribution, $P(\alpha)$, does just this. Ellenbroek and co-workers introduced the displacement angle α_{ij} [15]. Here α_{ij} denotes the angle between \mathbf{u}_{ij} and \mathbf{r}_{ij} (see Fig. 11), or,

$$\tan \alpha_{ij} = \frac{u_{\perp,ij}}{u_{||,ij}}. \quad (7)$$

Affine compression corresponds to a uniform shrinking of the bond vector between two particles, i.e. $u_{\perp,ij} = 0$ and $u_{||,ij} = -\epsilon r_{ij} \leq 0$, where ϵ is the magnitude of the applied strain on the system. In this scenario, $P(\alpha)$ exhibits a delta-function peak at $\alpha = \pi$. For affine shear, the effect depends on the bond vectors orientation, and for isotropic random packings, $P(\alpha)$ is flat.

In numerical simulations one finds that for large pressures, $P(\alpha)$ is not too dissimilar from the affine prediction, but that closer to point J, $P(\alpha)$ develops a substantial peak around $\pi/2$. These correspond to contacts where $u_{\perp} \gg u_{||}$ —in other words, to contacts, where the particles in essence slide past each other. Surprisingly, this peak develops and appears to diverge both for shear and compressive deformations [10,16].

In addition one can investigate the scaling of $u_{||}$ and u_{\perp} as well. The typical values of $u_{||}$ under a deformation are directly connected to the corresponding elastic modulus: for compression $u_{||}$ is essentially independent of the distance to jamming ($u_{||} \sim \epsilon$), while for shear, $u_{||} \sim \epsilon \Delta\phi^{1/4}$, where ϵ is the magnitude of the strain [11,16].

The scaling for u_{\perp} , the amount by which particles in contact slide past each other, is more subtle. Numerically, one observes that for shear deformations, $u_{\perp} \sim \epsilon \delta^{-1/4}$. The two terms $\propto u_{||}$ and $\propto u_{\perp}$ become comparable here, and the amount of sideways sliding under a shear deformation diverges near jamming [10,11,16]. For compression there is no simple scaling. Knowing that $\Delta z \sim \sqrt{\Delta\phi}$, the above expressions for $u_{||}$ and u_{\perp} , and guessing that in this case the two terms in Eq. (6) would balance, one might have expected $u_{\perp} \sim \epsilon \delta^{-1/2}$. However, the data suggest a weaker divergence, close to $\Delta\phi^{-0.3}$. Nevertheless, both under shear and compression, the sliding, sideways motion of contacting particles dominates and diverges near jamming.

The preceding findings illustrate the strange nature of linear response close to the jamming transition.

4.2. Contact number revisited

In this section, we are interested in the scaling of the contact number in greater detail. The (erroneous) linear prediction for the scaling of Δz with $\Delta\phi$ (Fig. 6(b)) stem from two assumptions: the system is affinely compressed and the gaps between

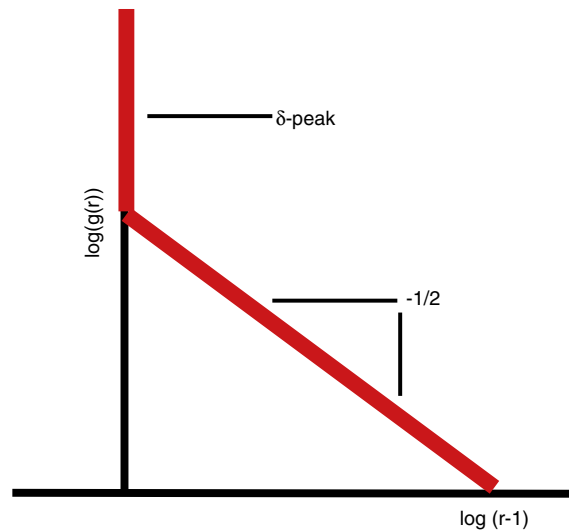


Fig. 12. Sketch of the pair correlation function $g(r)$ for monodisperse particles near jamming. Apart from a divergence as $1/\sqrt{r-1}$ which signifies that there are anomalously many very small gaps between particles, there is a δ -peak at $r = 1$, corresponding to the $nz/2$ particles that are precisely touching at jamming.

particles are evenly distributed. In the light of the discussion above, one might expect that the affine assumption is the culprit here. This appears not to be the case—the crux seems to be that the second assumption breaks down.

This breakdown can be quantified by the pair correlation function $g(r)$, which is the probability of finding two particles whose center points are separated by a distance r . For simplicity we only consider monodisperse systems of particles of diameter 1 here. The pair correlation function shows a squareroot divergence near $r = 1$ for systems close to jamming [17]—see Fig. 12. This divergence implies that there are anomalously many small gaps near jamming, and so even a small compression is expected to close many gaps. More precisely, the scaling of Δz can be related to the divergence of the radial distribution function, $g(r)$ [17]. We imagine a packing of spheres at point J. If the radii are increased in an affine way so that the overlap goes from zero to δ , it is reasonable to expect that such compression closes all gaps between particles that are smaller than δ . So

$$\Delta z \sim \int_1^{1+\delta} d\xi \frac{1}{\sqrt{\xi-1}} \sim \sqrt{\delta}, \quad (8)$$

where the integrand is the radial distribution function and $\xi = r/(R_i + R_j)$.

Note that the elastic discussion in Section 4.1 concerns the non-affine nature of the relative displacements of particles in contact, while the argument for Δz concerns particles *not yet* into contact—apparently the motion of these particles is not sufficiently non-affine to lead to corrections to scaling.

5. Summary and outlook

We have seen that soft frictionless spheres near the jamming transition exhibit a wealth of non-trivial and unexpected behavior. Their pair correlation function diverges, the response is strongly non-affine, the elastic moduli are anomalous and there is an excess of low frequency modes. Moreover, there appears to be a diverging length scale associated with the jamming of frictionless spheres. How generic is this behavior?

Recent studies of frictional particles [18] and elliptical particles [19,20] have shown that the contact number is absolutely key. In all these cases, the difference between the contact number and the relevant isostatic value (which is different for frictional and non-spherical particles) is crucial. However, not all systems reach the isostatic limit at the jamming transition—for example, the contact number in frictional systems remains typically above the isostatic value, and, correspondingly, the mechanical and geometric properties of these systems are less anomalous near jamming. It is thus useful to think of jamming as a two-step process. First, a packing with a certain contact number z is created for a given pressure. Second, the mechanical properties of the packing, such as elastic moduli and packing fraction, depend on the difference between the actual contact number and the relevant isostatic value. This isostatic contact number, as we have seen, is reached at the jamming threshold for frictionless spheres.

Important questions for the future is to extend the jamming framework to more general particle systems, and also to take the effect of shear and temperature into account. Moreover, despite the wealth of theoretical predictions, very few of these have been verified in experiment.

References

- [1] A.J. Liu, S.R. Nagel, *Nature* 396 (1998) 21.
- [2] M. van Hecke, *J. Phys. Cond. Matt.* 22 (2010) 033101.

- [3] A.J. Liu, S.R. Nagel, W. van Saarloos, M. Wyart, The Jamming scenario an introduction and outlook, 2010, preprint.
- [4] C.S. O'Hern, L.E. Silbert, A.J. Liu, S.R. Nagel, *Phys. Rev. E* 68 (2003) 011306.
- [5] M. Clusel, E. Corwin, A.O.N. Siemens, J. Brujic, *Nature* 460 (2009) 611.
- [6] C.F. Moukarzel, *Phys. Rev. Lett.* 81 (1998) 1634.
- [7] A.V. Tkachenko, T.A. Witten, *Phys. Rev. E* 60 (1999) 687.
- [8] D.J. Durian, *Phys. Rev. Lett.* 75 (1997) 4780.
- [9] H.A. Makse, N. Gland, D.L. Johnson, L.M. Schwartz, *Phys. Rev. Lett.* 83 (1999) 5070.
- [10] W.G. Ellenbroek, E. Somfai, M. van Hecke, W. van Saarloos, *Phys. Rev. Lett.* 97 (2006) 258001.
- [11] W.G. Ellenbroek, Z. Zeravcic, W. van Saarloos, M. van Hecke, *Europhys. Lett.* 87 (2009) 34004.
- [12] M. Wyart, L.E. Silbert, S.R. Nagel, T.A. Witten, *Phys. Rev. E* 72 (2005) 051306;
M. Wyart, *Ann. Phys. Fr.* 30 (2005) 1;
M. Wyart, S.R. Nagel, T.A. Witten, *Europhys. Lett.* 72 (2005) 486.
- [13] L.E. Silbert, A.J. Liu, S.R. Nagel, *Phys. Rev. Lett.* 95 (2005) 098301.
- [14] L.E. Silbert, A.J. Liu, S.R. Nagel, *Phys. Rev. E* 79 (2009) 021308.
- [15] Not to be confused by the power law index of the interaction potential.
- [16] W.G. Ellenbroek, M. van Hecke, W. van Saarloos, 2009, accepted for PRE.
- [17] L.E. Silbert, A.J. Liu, S.R. Nagel, *Phys. Rev. E* 73 (2006) 041304.
- [18] E. Somfai, M. van Hecke, W.G. Ellenbroek, K. Shundyak, W. van Saarloos, *Phys. Rev. E* 75 (2007) 020301(R).
- [19] M. Mailman, C.F. Schreck, C.S. O'Hern, B. Chakraborty, *Phys. Rev. Lett.* 102 (2009) 255501.
- [20] Z. Zeravcic, N. Xu, A.J. Liu, S.R. Nagel, W. van Saarloos, *Europhys. Lett.* 87 (2009) 26001.